Bifurcations and chaotic threshold for a nonlinear system with an irrational restoring force*

Tian Rui-Lan(田瑞兰)[a], Yang Xin-Wei(杨新伟)[b],
Cao Qing-Jie(曹庆杰)[c]†, and Wu Qi-Liang(吴启亮)[a]

[a] *Department of Mathematics and Physics, Shijiazhuang Tiedao University, Shijiazhuang* 050043, *China*
[b] *School of Traffic, Shijiazhuang Institute of Railway Technology, Shijiazhuang* 050041, *China*
[c] *School of Astronautics, Harbin Institute of Technology, Harbin* 150001, *China*

(Received 30 August 2011; revised manuscript received 2 October 2011)

Nonlinear dynamical systems with an irrational restoring force often occur in both science and engineering, and always lead to a barrier for conventional nonlinear techniques. In this paper, we have investigated the global bifurcations and the chaos directly for a nonlinear system with irrational nonlinearity avoiding the conventional Taylor's expansion to retain the natural characteristics of the system. A series of transformations are proposed to convert the homoclinic orbits of the unperturbed system to the heteroclinic orbits in the new coordinate, which can be transformed back to the analytical expressions of the homoclinic orbits. Melnikov's method is employed to obtain the criteria for chaotic motion, which implies that the existence of homoclinic orbits to chaos arose from the breaking of homoclinic orbits under the perturbation of damping and external forcing. The efficiency of the criteria for chaotic motion obtained in this paper is verified via bifurcation diagrams, Lyapunov exponents, and numerical simulations. It is worthwhile noting that our study is an attempt to make a step toward the solution of the problem proposed by Cao Q J *et al.* (Cao Q J, Wiercigroch M, Pavlovskaia E E, Thompson J M T and Grebogi C 2008 *Phil. Trans. R. Soc.* A **366** 635).

Keywords: nonlinear dynamical system, Melnikov boundary, irrational restoring force, saddle-like singularity, homoclinic-like orbit

PACS: 05.45.–a, 05.45.Ac, 82.40.Bj **DOI:** 10.1088/1674-1056/21/2/020503

1. Introduction

Strongly nonlinear systems governed by irrational restoring forces have attracted the attention of researchers,[1−7] and are widely used in physics and engineering. Unfortunately, an irrational restoring force is a barrier to detecting the nonlinear dynamics in classical methodologies, as is the open problem mentioned in Ref. [1] for the recently proposed smooth-and-discontinuous (SD) oscillator.[1,8,9] Conventionally, Taylor-series approaches are often used to simplify nonlinearities into a Taylor series. See for example, the codimension-two bifurcation of the SD oscillator that was analysed using the Taylor expansion near the critical value of $\alpha = 1$;[10] the response of a harmonically excited two-degree-of-freedom system consisting of a linear and a nonlinear quasi-zero stiffness oscillators was detected.[11,12] However, this expansion is invalid or does not meet the requirements of the study, which means that the classical methodologies are not effective in the investigation of nonlinear dynamics for this kind of system. In fact, the Taylor-series expansion of nonlinear restoring force $G(x) = -x\left(1 - 1/\sqrt{x^2+\alpha^2}\right)$ is valid only for $\alpha > 0$ and fails for $\alpha = 0$.[1,8] Therefore, effective methodologies to study this kind of nonlinear system need to be developed. The improved harmonic balance method[13] and the homotopy perturbation methods[14] have been applied to detect the oscillation of mass attached to a stretched wire. The trilinear approach[8] was introduced to study the chaos of an SD oscillator. An averaging technique is employed to obtain Hopf bifurcation for an SD oscillator (cf. Ref. [15]).

The motivation of this paper is to explore the chaotic behaviours of systems with an irrational restoring force directly to the irrationalities, avoiding the conventional Taylor's expansion to retain the intrinsic characteristics of the system. By means of

*Project supported by the National Natural Science Foundation of China (Grant Nos. 11002093, 11072065, and 10872136) and the Science Foundation of the Science and Technology Department of Hebei Province of China (Grant No. 11215643).

†Corresponding author. E-mail: caoqingjie@hotmail.com

© 2012 Chinese Physical Society and IOP Publishing Ltd

the analytical expressions of the homoclinic orbits, the Melnikov procedure can be directly used in the irrational systems to detect the original behaviour of the system. Furthermore, this investigation forwards the open problem in Ref. [1].

This paper is organized as follows. In the next section, the equations of motion are given and the Hamiltonian function including an irrational term is derived: it is not readily analysed. In Section 3, the equilibria of the system are detected depending on the value of the parameters α and λ. Phase portraits of the system that is unperturbed (undamped and undriven) are detected. In addition, a kind of transformations is introduced and the expressions for the homoclinic orbits are developed. This approach is valid for both smooth and limited discontinuous systems. In Section 4, the Melnikov method is applied to determine the distance between the stable and unstable manifolds. Bifurcation diagrams and Lyapunov exponents are then considered. Numerical simulations are also carried out in Section 5, which confirm these analytical predictions.

2. Preliminary dynamic analysis

An ordinary differential equation[2] is governed by

$$\frac{\mathrm{d}^2u}{\mathrm{d}t^2} + f(u) = 0, \tag{1}$$

in which the irrational restoring force function $-f(u)$ is given by

$$-f(u) = -\omega_0^2 u\left(1 - \frac{\lambda}{\sqrt{u^2+\alpha^2}}\right), \tag{2}$$

where u, t, ω_0, $0 < \lambda \leq 1$, and $\alpha \geq 0$ are, respectively, the dimensionless displacement, time variable, the natural frequency, the stretch parameter,[13] and the smoothness parameter.[1] When $u(0) = A$, $\mathrm{d}u(0)/\mathrm{d}t = 0$, a generalized Senator–Bapat perturbation technique is employed to deal with the approximate solution of this nonlinear system. The reader can refer to Ref. [2] for further details.

Now suppose system (1) has viscous damping, an external harmonic excitation of amplitude F and frequency Ω. For convenience, let $\omega_0^2 = 1$. These values lead to a forced dissipative oscillator of the following form

$$\frac{\mathrm{d}^2u}{\mathrm{d}t^2} + \xi\dot{u} + u(1 - \frac{\lambda}{\sqrt{u^2+\alpha^2}}) = F\cos\Omega t. \tag{3}$$

This system can be smooth or discontinuous depending on the value of the smoothness parameter α, as shown in Fig. 1. With the change of the parameters α and λ, system (3) corresponds to different mathematical models. Especially, when $\lambda = 1$, the system is just an SD system.

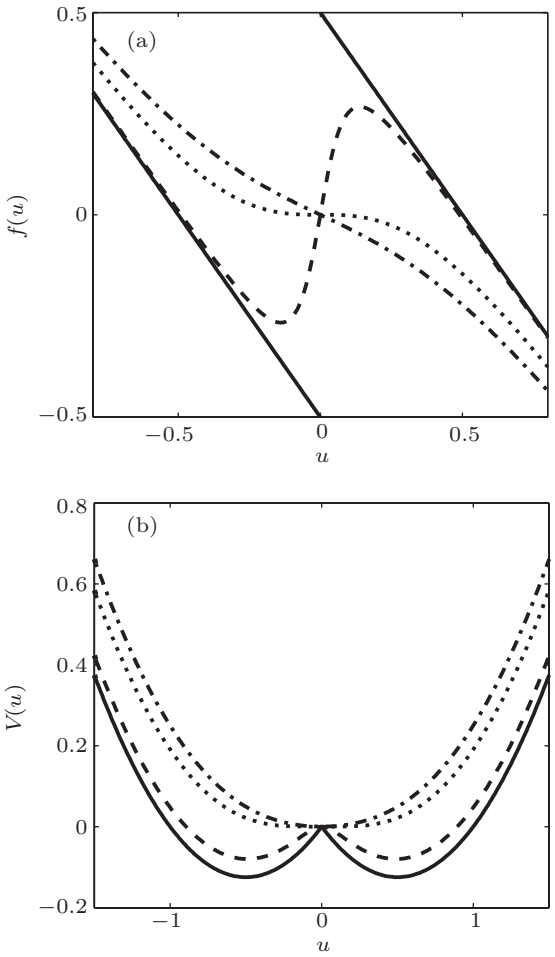


Fig. 1. (a) Restoring forces and (b) potential function $V(u) = \frac{1}{2}u^2 - \lambda\sqrt{u^2+\alpha^2} + \lambda\alpha$ for $\lambda = 0.6$. The solid curves are for $\alpha = 0$, the dashed curves are for $\alpha = 0.1$, the dotted curves are for $\alpha = 0.5$, the dot-dashed curves are for $\alpha = 0.75$.

Equation (3) can be written as two first order differential equations by letting $\mathrm{d}u/\mathrm{d}t = v$

$$\begin{aligned} \dot{u} &= v, \\ \dot{v} &= -\xi v - u\left(1 - \frac{\lambda}{\sqrt{u^2+\alpha^2}}\right) + F\cos\Omega t, \end{aligned} \tag{4}$$

where $\dot{u} = \mathrm{d}u/\mathrm{d}t$, $\dot{v} = \mathrm{d}^2u/\mathrm{d}t^2$.

The scale transformations may be introduced as follows:

$$\xi \to \varepsilon\xi,\ F \to \varepsilon F. \tag{5}$$

Then equation (4) can be rewritten in the following

form with the perturbation

$$\begin{aligned}\dot{u} &= \frac{\partial H}{\partial v} + \varepsilon g_1 = v,\\ \dot{v} &= -\frac{\partial H}{\partial u} + \varepsilon g_2\\ &= -u\left(1 - \frac{\lambda}{\sqrt{u^2+\alpha^2}}\right) + \varepsilon(-\xi v + F\cos\Omega t), \quad (6)\end{aligned}$$

where the Hamiltonian function is of the form

$$H(u,v) = \frac{1}{2}v^2 + \frac{1}{2}u^2 - \lambda\sqrt{u^2+\alpha^2} + \lambda\alpha, \quad (7)$$

$$g_1 = 0, g_2 = -\xi v + F\cos\Omega t. \quad (8)$$

It is noted that Hamiltonian function $H(u,v)$ includes an irrational term, which cannot meet the requirements of the conventional methods. Hence, it leads to many barriers to detecting the dynamics, which will be investigated in the following sections.

3. The dynamics of an unperturbed system

For $\varepsilon = 0$, equation (6) takes the form

$$\begin{aligned}\dot{u} &= v,\\ \dot{v} &= -u\left(1 - \frac{\lambda}{\sqrt{u^2+\alpha^2}}\right), \quad (9)\end{aligned}$$

which describes an undamped and undriven oscillator. Clearly, the equilibria of system (9) depend on the values of α and λ and they are

$$(0,0), (\pm\sqrt{\lambda^2-\alpha^2}, 0). \quad (10)$$

To examine the influence of parameters of α and λ on the dynamics of Eq. (9), we construct the bifurcation diagram, depicted in Fig. 2(a). The system undergoes a bifurcation at $\alpha - \lambda = 0$ where the stable branch $u = 0$ bifurcates into two stable branches at $u = \pm\sqrt{\lambda^2-\alpha^2}$. The stationary $u = 0$ state is now unstable, exhibiting the standard hyperbolic structure. Especially, $u = 0$ is not a fixed point because u yields $u \neq 0$ in Eq. (9) when $\alpha = 0$ and system (9) becomes a discontinuous system. Hence, for system (9), it is possible to study global bifurcations in the (α, λ) parameter plane as shown in Fig. 2(b), where four regions exist as follows:

$$\text{(I) } 0 < \lambda < \alpha; \qquad \text{(II) } \lambda = \alpha > 0;$$

$$\text{(III) } \lambda > \alpha > 0; \qquad \text{(IV) } \lambda > \alpha = 0.$$

Each of these regions have different qualitative flow behaviours (see Fig. 3) and they are described below.

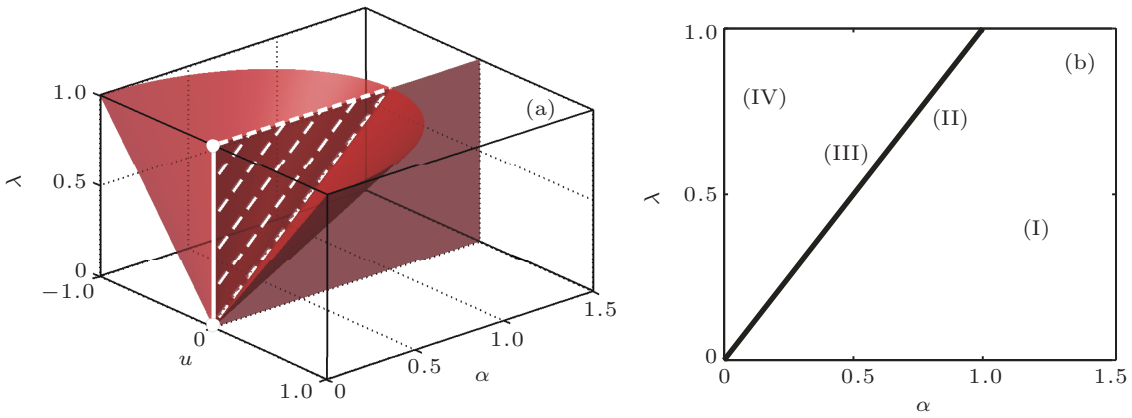


Fig. 2. (colour online) Bifurcation diagram of unperturbed system (9): (a) u–α–λ; (b) α–λ.

Region (I): Nonlinear system (9) has the only centre (0,0) (see Fig. 3(a)), which may introduce Hopf bifurcation[15–17] and can be carried out using method similar to that used in Ref. [15].

Region (II): the origin is the only fixed point (see Fig. 3(b)), which is non-hyperbolic. The case may introduce codimension-two bifurcation, which can be investigated by applying a similar method to that used in Ref. [6].

Region (III): there exist three fixed points. The origin is a saddle and $(\pm\sqrt{\lambda^2-\alpha^2}, 0)$ are centre equilibria, (see Fig. 3(c)).

Region (IV): nonlinear system (9) has two centres $(\pm\lambda, 0)$. Note that the origin is not a fixed point. However, the behaviour of the flow near (0,0) is similar to the saddle. Hence, it is called a saddle-like singularity in Ref. [1], (see Fig. 3(d)).

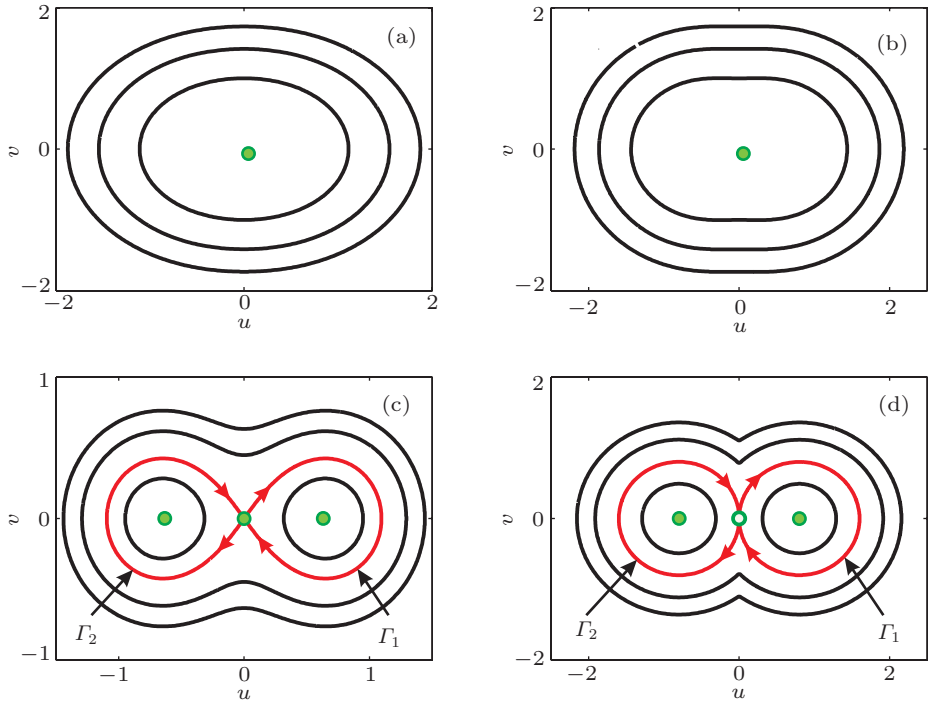


Fig. 3. (colour online) Phase portraits in the u–v plane for the unperturbed system (9): (a) region (I) in Fig. 2(b); (b) region (II) in Fig. 2(b); (c) region (III) in Fig. 2(b); (d) region (IV) in Fig. 2(b).

From Fig. 3(c), it is clear that the origin is connected to itself by a pair of symmetric homoclinic orbits $\Gamma_{1,2} = (u_{1,2}, v_{1,2})$, each of which satisfies

$$\frac{1}{2}{v_{1,2}}^2 + \frac{1}{2}{u_{1,2}}^2 - \lambda\sqrt{{u_{1,2}}^2 + \alpha^2} + \lambda\alpha = 0. \quad (11)$$

From Fig. 3(d), we know that a saddle-like singularity is taken as connecting to itself by the special homoclinic-like orbits[1] $\Gamma_{1,2} = (u_{1,2}, v_{1,2})$, each of which yields Eq. (11). In this paper, we are interested in regions (III) and (IV). However, equation (11) is not readily analysed directly. Obviously, the barriers are similar to the ones proposed in Ref. [1]. In this paper, introducing a series of transformations[18,19]

$$\begin{aligned} u &= \sqrt{2B}\cos\theta, \\ v &= \sqrt{2B}\sin\theta, \quad (B \geq 0), \end{aligned} \quad (12)$$

we will consider the homoclinic orbits.

Clearly,

$$\begin{aligned} \dot{B} &= \sqrt{2B}(\dot{u}\cos\theta + \dot{v}\sin\theta), \\ \sqrt{2B}\dot{\theta} &= \dot{v}\cos\theta - \dot{u}\sin\theta. \end{aligned} \quad (13)$$

So, unperturbed equation (9) becomes

$$\begin{aligned} \dot{B} &= \frac{2B\lambda\cos\theta\sin\theta}{\sqrt{2B\cos^2\theta + \alpha^2}}, \\ \dot{\theta} &= -1 + \frac{\lambda\cos^2\theta}{\sqrt{2B\cos^2\theta + \alpha^2}}; \end{aligned} \quad (14)$$

and the Hamiltonian $H(u, v)$ is transformed into

$$H(B, \theta) = B - \lambda\sqrt{2B\cos^2\theta + \alpha^2} + \lambda\alpha. \quad (15)$$

Obviously, the periodic time of system (14) is π. So, we can choose $-\pi/2 \leq \theta \leq \pi/2$, which leads to the study of homoclinic orbit Γ_1 from transformation (12). When we choose $\pi/2 \leq \theta \leq 3\pi/2$, the homoclinic orbits Γ_2 will be considered.

In phase space $(B,\ \theta)$, when $\lambda > \alpha \geq 0$, all possible fixed points are

$$(0, \pm\theta^*),\ (B^*, 0), \quad (16)$$

or

$$(0, \pi \pm \theta^*), (B^*, \pi), \quad (17)$$

where $\theta^* = \arccos\sqrt{\alpha/\lambda}$, $B^* = (\lambda^2 - \alpha^2)/2$.

Note that $(0, \pm\theta^*)$ (or $(0, \pi \pm \theta^*)$) are saddles, and $(B^*, 0)$ (or (B^*, π)) is a centre. From Fig. 4, we know that every phase portrait contains two heteroclinic orbits A and A' (C and C') and the points in the two heteroclinic orbits satisfy

$$\cos^2\theta \geq \frac{\alpha}{\lambda}. \quad (18)$$

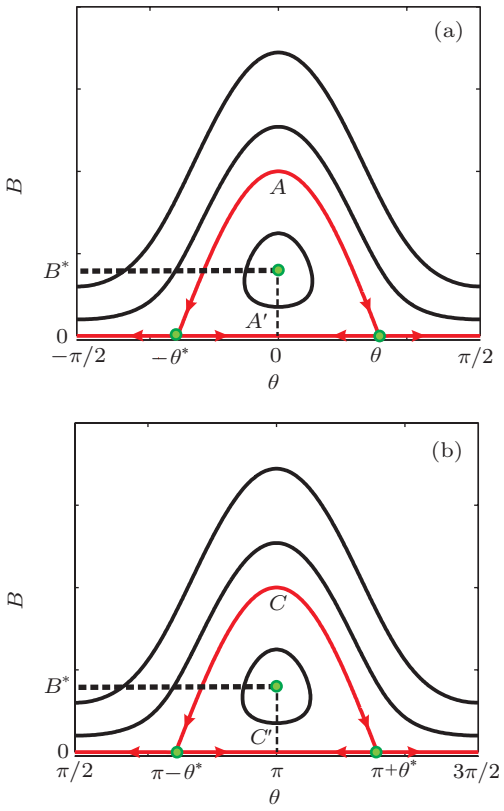


Fig. 4. (colour online) Phase portraits of system (14) when $\lambda > \alpha \geq 0$: (a) $-\pi/2 \leq \theta \leq \pi/2$; (b) $\pi/2 \leq \theta \leq 3\pi/2$.

By continuity, the homoclinic orbits given in Eq. (11) yield

$$H(B,\theta) = H(0,\theta), \tag{19}$$

from which we obtain

$$A(C) : B = 2\lambda^2\cos^2\theta - 2\lambda\alpha, \tag{20}$$

$$A'(C') : B = 0. \tag{21}$$

Firstly, consider heteroclinic $A(C)$. Substituting Eq. (20) into the $\dot{\theta}$ component of Eq. (14) leads to

$$\dot{\theta} = -1 + \frac{\lambda\cos^2\theta}{|2\lambda\cos^2\theta - \alpha|}. \tag{22}$$

From Eq. (18), we obtain the following equation

$$\dot{\theta} = -1 + \frac{\lambda\cos^2\theta}{2\lambda\cos^2\theta - \alpha}. \tag{23}$$

Integrating the expression for $\dot{\theta}$ under the initial condition $\theta(0) = 0$ satisfies

$$\varphi(\theta) = t, \tag{24}$$

where

$$\varphi(\theta) = -2\theta - \frac{\sqrt{\alpha}}{2\sqrt{\lambda-\alpha}} \times \ln\frac{\sqrt{\lambda-\alpha}\cos\theta + \sqrt{\alpha}\sin\theta}{\sqrt{\lambda-\alpha}\cos\theta - \sqrt{\alpha}\sin\theta}. \tag{25}$$

Secondly, for heteroclinic orbits $A'(C')$, we have

$$\dot{\theta} = -1 + \frac{\lambda}{\alpha}\cos^2\theta. \tag{26}$$

Hence, under the initial condition $\theta(0) = 0$, θ is described as

$$\theta(t) = \arctan\left\{\sqrt{\frac{\lambda}{\alpha} - 1}\tanh\sqrt{\frac{\lambda}{\alpha} - 1}t\right\}. \tag{27}$$

Note that from Eqs. (12), (21), and (27), the homoclinic orbits can be obtained

$$\begin{aligned} u_{1,2} &= 0, \\ v_{1,2} &= 0. \end{aligned} \tag{28}$$

In fact, the homoclinic orbit is the origin of system (9). Hence, the homoclinic orbits $\Gamma_{1,2}$ of Eq. (11) satisfy

$$\begin{aligned} u_{1,2} &= 2\sqrt{\lambda^2\cos^2\theta - \lambda\alpha}\cos\theta, \\ v_{1,2} &= 2\sqrt{\lambda^2\cos^2\theta - \lambda\alpha}\sin\theta, \end{aligned} \tag{29}$$

where θ yields Eq. (24) and $-\pi/2 \leq \theta \leq \pi/2$ (or $\pi/2 \leq \theta \leq 3\pi/2$).

In particular, when $\lambda = 1$, system (9) becomes an SD oscillator, and the homoclinic orbits take the following form

$$\begin{aligned} u_{1,2} &= 2\sqrt{\cos^2\theta - \alpha}\cos\theta, \\ v_{1,2} &= 2\sqrt{\cos^2\theta - \alpha}\sin\theta, \end{aligned} \tag{30}$$

where θ can be given as

$$-2\theta - \frac{\sqrt{\alpha}}{2\sqrt{1-\alpha}}\ln\frac{\sqrt{1-\alpha}\cos\theta + \sqrt{\alpha}\sin\theta}{\sqrt{1-\alpha}\cos\theta - \sqrt{\alpha}\sin\theta} = t, \tag{31}$$

and $-\pi/2 \leq \theta \leq \pi/2$ (or $\pi/2 \leq \theta \leq 3\pi/2$).

When $\lambda = 1$ and $\alpha = 0$, from Eq. (24), we can obtain $\theta = -t/2$, i.e., the limited discontinuous system of SD oscillator, then homoclinic orbits become

$$\begin{aligned} u_{1,2} &= \pm 2\cos^2\frac{t}{2}, \\ v_{1,2} &= \mp 2\cos\frac{t}{2}\sin\frac{t}{2}. \end{aligned} \tag{32}$$

The results mentioned above might imply a further step towards solving the open SD oscillator problem in Ref. [1].

4. Dynamics of the perturbed system

In this section, we focus our attention on the existence of chaos[20−25] in Eq. (6). The Melnikov method will be used to detect the homoclinic tangency (the Melnikov boundary) beyond which chaos may be generated. Subsequently, the bifurcation diagrams and the Lyapnnov exponents diagrams are investigated.

The Melnikov function[26−28] is given by

$$M_{1,2}(t_0) = \int_{-\infty}^{+\infty} f(\Gamma_{1,2}) \Lambda g(\Gamma_{1,2}, t+t_0)\,\mathrm{d}t, \quad (33)$$

where

$$f(\Gamma_{1,2}) = \begin{pmatrix} \dfrac{\partial H}{\partial v}(\Gamma_{1,2}) \\ -\dfrac{\partial H}{\partial u}(\Gamma_{1,2}) \end{pmatrix},$$

$$g(\Gamma_{1,2}, t+t_0) = \begin{pmatrix} g_1(\Gamma_{1,2}, t+t_0) \\ g_2(\Gamma_{1,2}, t+t_0) \end{pmatrix},$$

and the operator Λ is defined as

$$a \Lambda b = a_1 b_2 - a_2 b_1 \quad (34)$$

for any $a = (a_1, a_2)^{\mathrm{T}}$ and $b = (b_1, b_2)^{\mathrm{T}}$.

From Eqs. (7), (8), (12), (24), (29), and (33), we have

$$\begin{aligned} M_1(t_0) &= \int_{-\infty}^{+\infty} [-\xi v_1^2 + v_1 F \cos \Omega(t+t_0)]\,\mathrm{d}t \\ &= \int_{-\infty}^{+\infty} [-\xi v_1 + F \cos \Omega(t+t_0)]\,\mathrm{d}(u_1) \\ &= \int_{-\infty}^{+\infty} [-\xi \sqrt{2B} \sin\theta + F \cos \Omega(t+t_0)] \\ &\quad \times \mathrm{d}(\sqrt{2B}\cos\theta) \\ &= \int_{-\theta^*}^{\theta^*} [-\xi \sqrt{2B} \sin\theta + F \cos \Omega(t+t_0)] \\ &\quad \times \left[\frac{-4\lambda^2 \cos^2\theta \sin\theta}{\sqrt{2B}} - \sqrt{2B}\sin\theta\right] \mathrm{d}\theta \\ &= 8\xi\lambda^2\varphi_1 - 4\lambda\xi\alpha\varphi_2 - F\sin(\Omega t_0)\varphi_3, \quad (35) \end{aligned}$$

where

$$\begin{aligned} \varphi_1 &= \int_{-\theta^*}^{\theta^*} \cos^2\theta \sin^2\theta\,\mathrm{d}\theta, \\ \varphi_2 &= \int_{-\theta^*}^{\theta^*} \sin^2\theta\,\mathrm{d}\theta, \\ \varphi_3 &= \int_{-\theta^*}^{\theta^*} \sin(\varphi(\theta)\Omega) \\ &\quad \times \left[\frac{-4\lambda^2 \cos^2\theta \sin\theta}{\sqrt{2B}} - \sqrt{2B}\sin\theta\right] \mathrm{d}\theta. \quad (36) \end{aligned}$$

Furthermore,

$$\begin{aligned} M_2(t_0) &= \int_{-\infty}^{+\infty} [-\xi v_2^2 + v_2 F \cos \Omega(t+t_0)]\,\mathrm{d}t \\ &= 8\xi\lambda^2\varphi_1 - 4\lambda\xi\alpha\varphi_2 - F\sin(\Omega t_0)\varphi_4, \quad (37) \end{aligned}$$

where

$$\begin{aligned} \varphi_4 &= \int_{-\theta^*+\pi}^{\theta^*+\pi} \sin(\varphi(\theta)\Omega) \\ &\quad \times \left[\frac{-4\lambda^2 \cos^2\theta \sin\theta}{\sqrt{2B}} - \sqrt{2B}\sin\theta\right] \mathrm{d}\theta. \end{aligned}$$

It can be seen that

$$M_1(t_0) = 0 \quad (38)$$

has a simple zero for t_0 if and only if the following inequality holds

$$F > \left| \frac{8\xi\lambda^2\varphi_1 - 4\lambda\xi\alpha\varphi_2}{\varphi_3} \right|. \quad (39)$$

Similarly,

$$M_2(t_0) = 0 \quad (40)$$

has a simple zero for t_0 if and only if the following inequality holds

$$F > \left| \frac{8\xi\lambda^2\varphi_1 - 4\lambda\xi\alpha\varphi_2}{\varphi_4} \right|. \quad (41)$$

To conclude, the Melnikov boundary of Eq. (6) should be satisfied

$$\begin{aligned} F > \min\Bigg\{ &\left| \frac{8\xi\lambda^2\varphi_1 - 4\lambda\xi\alpha\varphi_2}{\varphi_3} \right|, \\ &\left| \frac{8\xi\lambda^2\varphi_1 - 4\lambda\xi\alpha\varphi_2}{\varphi_4} \right| \Bigg\}, \quad (42) \end{aligned}$$

beyond which chaos will be generated.

The Melnikovian detected chaotic boundary from Eq. (6) is obtained at $\alpha = 0$, as shown in Fig. 5(a) and at $\alpha = 0.2$ as shown in Fig. 5(b) for different values of parameters $\lambda = 1,\ 0.8,\ 0.6$. Chaotic motion exists in the area beyond the boundaries. Furthermore, the bifurcation diagrams under controlled variation of the amplitude F of the external excitation are shown in Fig. 6 for $\lambda = 0.6$, $\xi = 0.05$, $\Omega = 1.15$, (a) $\alpha = 0$ and (b) $\alpha = 0.2$; the corresponding Lyapnnov exponent diagrams are shown in Fig. 6 for $\lambda = 0.6$, (c) $\alpha = 0$ and (d) $\alpha = 0.2$. As can be seen in Fig. 6, no chaotic motion is observed below the boundary predicted by Melnikov method, which is marked by the dashed lines. From Fig. 6, a good degree of correlation is obtained both in the bifurcation diagrams (see Figs. 6(a) and (b)) and in the Lyapnnov exponents diagrams (see Figs. 6(c) and (d)) for both the smooth and the limited discontinuous system.

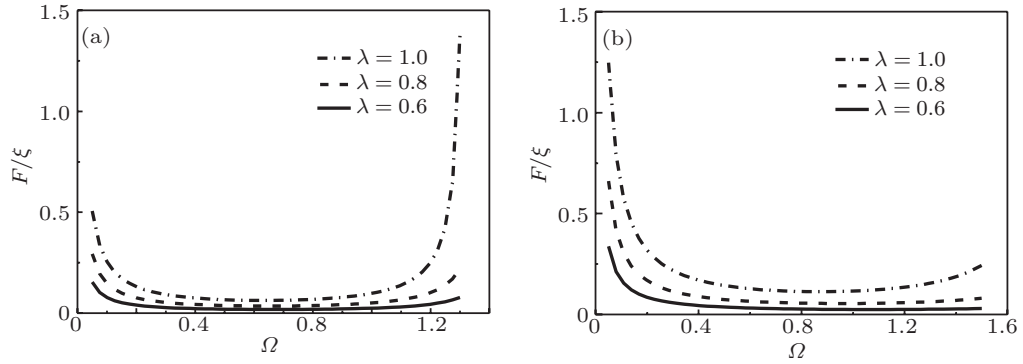


Fig. 5. Chaotic boundaries for system (6) detected by using the Melnikov method: (a) $\alpha = 0$; (b) $\alpha = 0.2$.

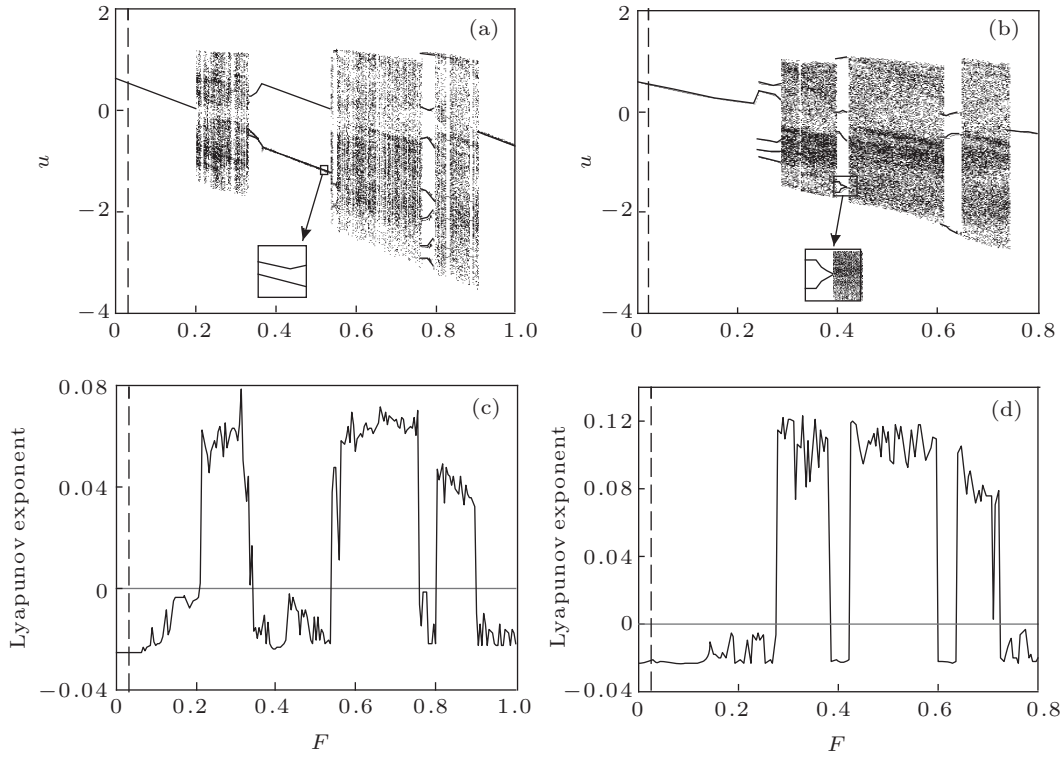


Fig. 6. Bifurcation diagrams for displacement u versus the external forcing amplitude F for $\lambda = 0.6$, $\xi = 0.05$, $\Omega = 1.15$: (a) $\alpha = 0$, and (b) $\alpha = 0.2$; Lyapunov exponent versus F: (c) $\alpha = 0$, and (d) $\alpha = 0.2$.

5. Numerical simulation

In this section, by using the numerical method, the cases for Figs. 5 and 6 are verified and the chaotic motion of system (6) is studied. The dynamics that present the non-chaotic response below the Melnikov boundary is shown in Figs. 7 and 8. Although all the chosen parameters yield inequality (42), chaotic motion does not exist, as shown in Figs. 9–12. In addition, the chaotic responses beyond the Melnikov boundary are shown in Figs. 13 and 14 for both smooth and discontinuous phenomena. The following diagrams represent the phase portraits (see Figs. 7(a)–14(a)), the projection of the Poincaré map (see Figs. 7(b)–14(b)) and the time-history portraits (see Figs. 7(c) and 7(d)–Figs. 14(c) and 14(d)). Parameters are chosen as $\lambda = 0.6$, $\xi = 0.05$, $\Omega = 1.15$. Specifically, the numerical results indicate that there exist three interesting cases and the details are described as follows.

(i) When $\alpha = 0$, we obtain the existence of period-1 motion due to the forcing excitation $F = 0.03$, as shown in Fig. 7. As $\alpha = 0.2$, the existence of the period-1 motion due to the forcing excitation $F = 0.02$ is shown in Fig. 8. Clearly, inequality (42) does not hold due to all the chosen parameters, which denotes that no chaotic motions can exist.

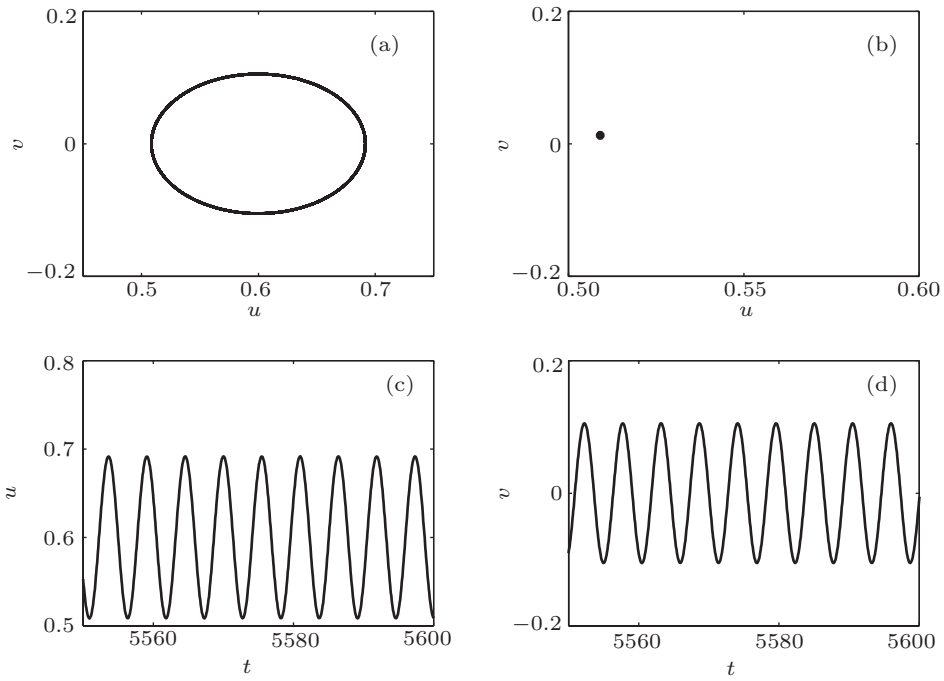


Fig. 7. The period-1 motion for $\alpha = 0$, $\lambda = 0.6$, $\xi = 0.05$, $\Omega = 1.15$, $F = 0.03$.

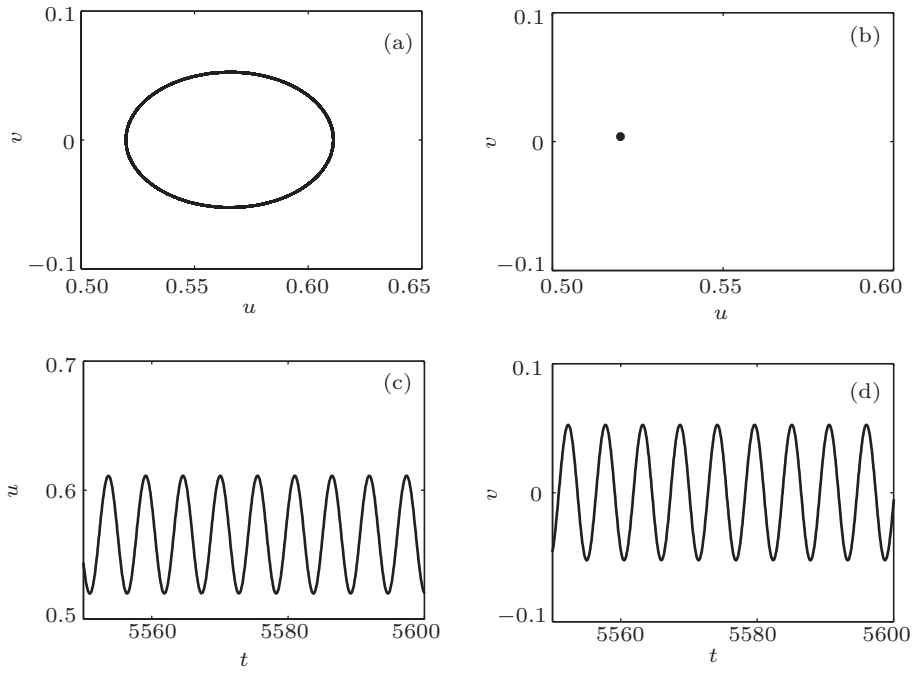


Fig. 8. The period-1 motion for $\alpha = 0.2$, $\lambda = 0.6$, $\xi = 0.05$, $\Omega = 1.15$, $F = 0.02$.

(ii) When $\alpha = 0$, we can show the existence of period-3 motion ($F = 0.43$) and period-7 motion ($F = 0.77$), as shown in Figs. 9 and 10, respectively. While $\alpha = 0.2$, the period-4 motion for $F = 0.416$ and the period-5 motion for $F = 0.23$ are shown in Figs. 11 and 12, respectively. In this case, although inequality (42) holds, no chaotic motions can exist, which confirms that the Melnikovian detected chaotic boundary is the necessary and insufficient condition for chaos.

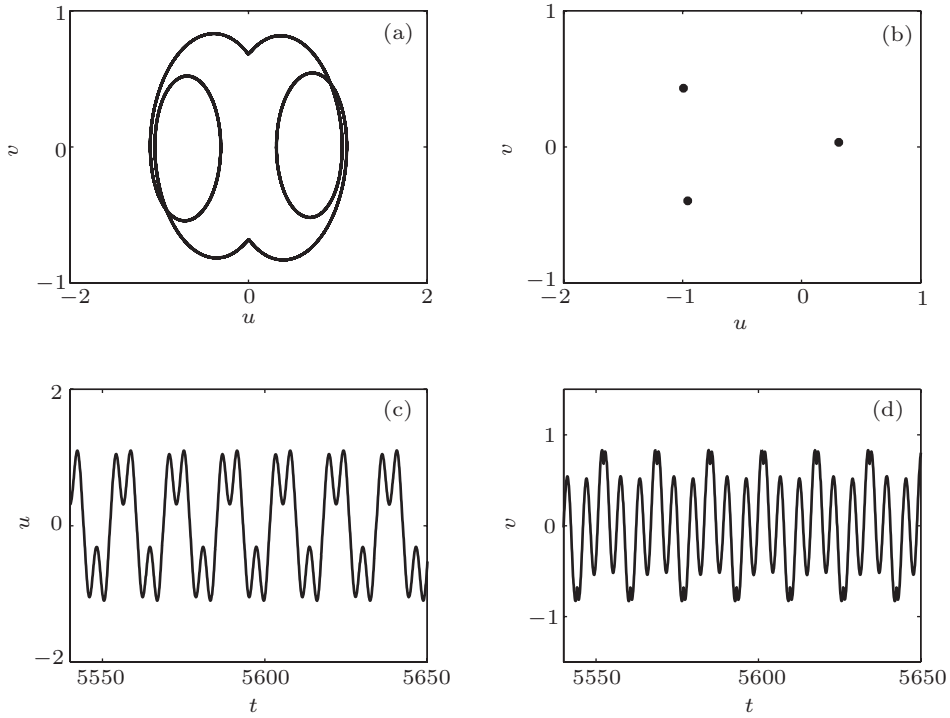


Fig. 9. The period-3 motion for $\alpha = 0$, $\lambda = 0.6$, $\xi = 0.05$, $\Omega = 1.15$, $F = 0.43$.

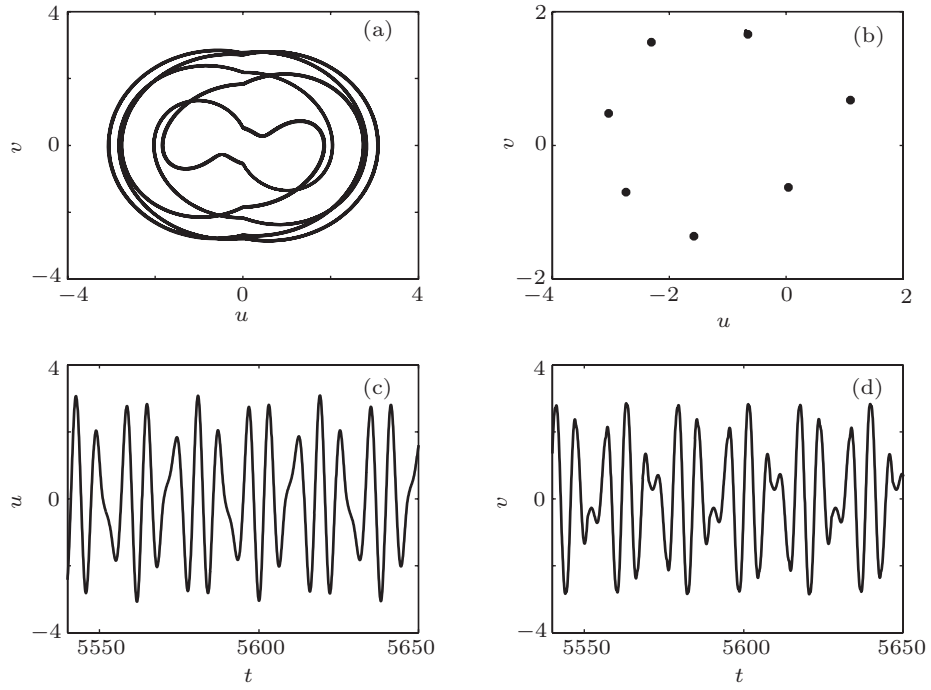


Fig. 10. The period-7 motion for $\alpha = 0$, $\lambda = 0.6$, $\xi = 0.05$, $\Omega = 1.15$, $F = 0.77$.

(iii) The chaotic attractor is presented in Fig. 13 ($\alpha = 0$ and $F = 0.6$) and Fig. 14 ($\alpha = 0.2$ and $F = 0.5$), respectively. Obviously, inequality (42) is found for the chosen parameters. As can be seen in Fig. 14, the structure of the attractor differs significantly from the one obtained in Fig. 13.

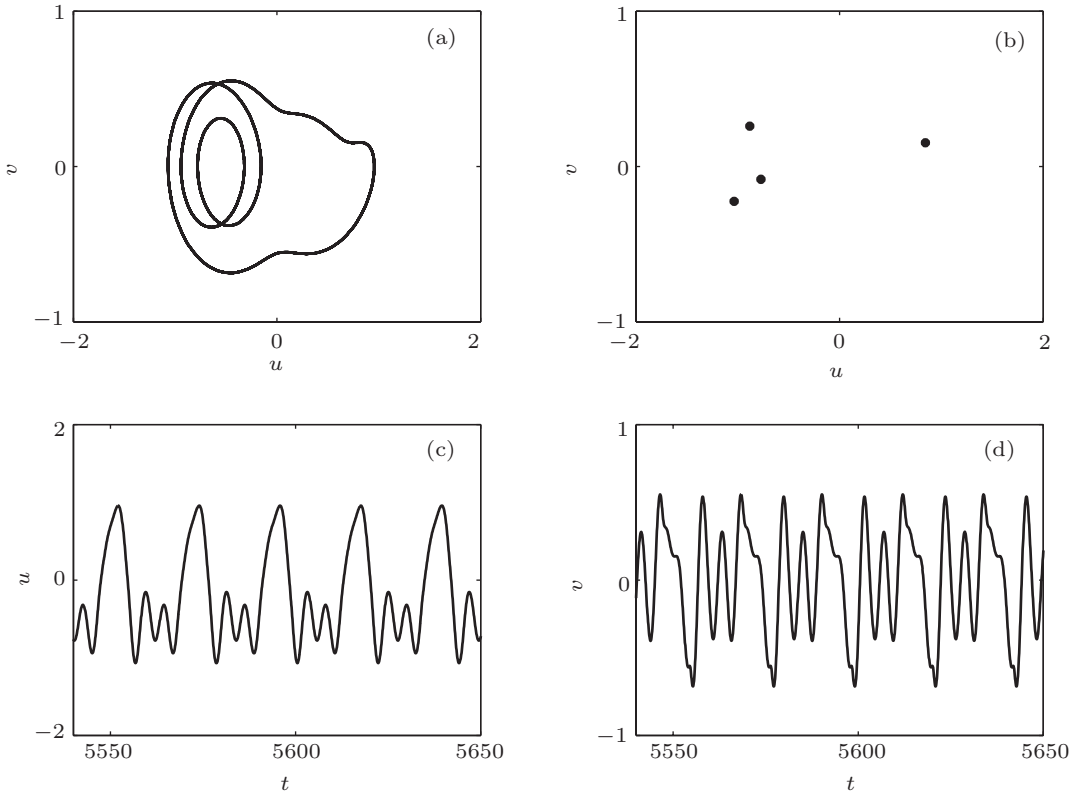


Fig. 11. The period-4 motion for $\alpha = 0.2$, $\lambda = 0.6$, $\xi = 0.05$, $\Omega = 1.15$, $F = 0.416$.

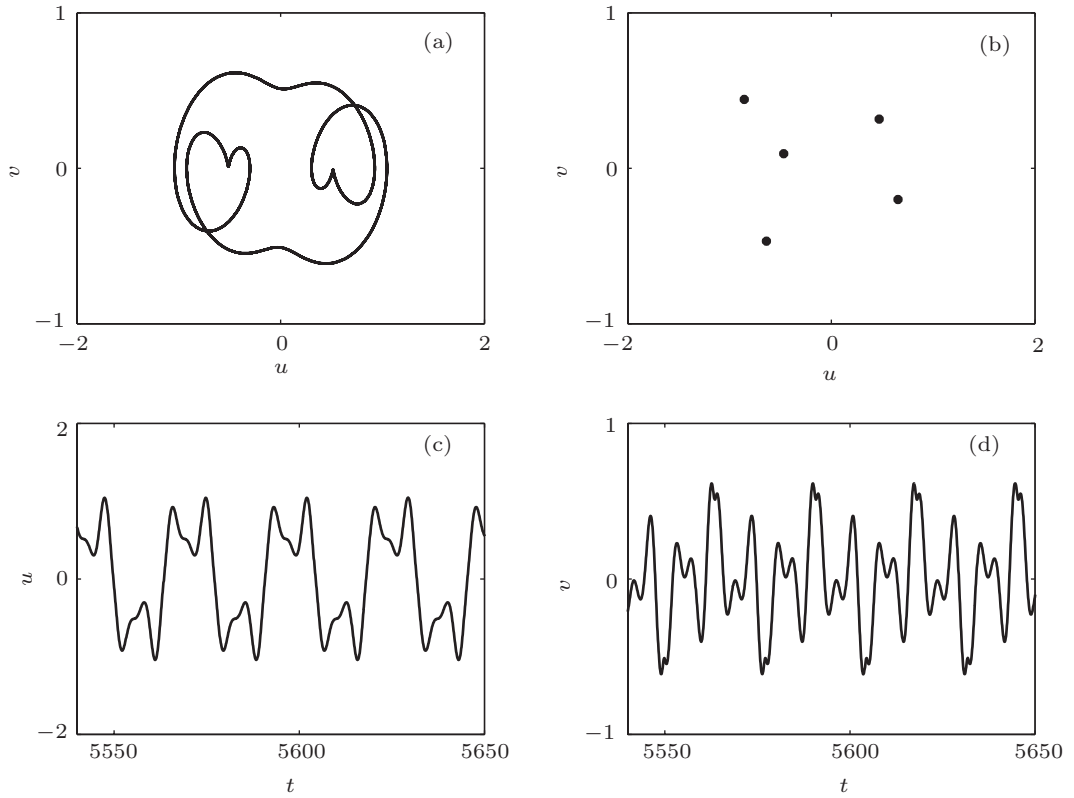


Fig. 12. The period-5 motion for $\alpha = 0.2$, $\lambda = 0.6$, $\xi = 0.05$, $F = 0.23$.

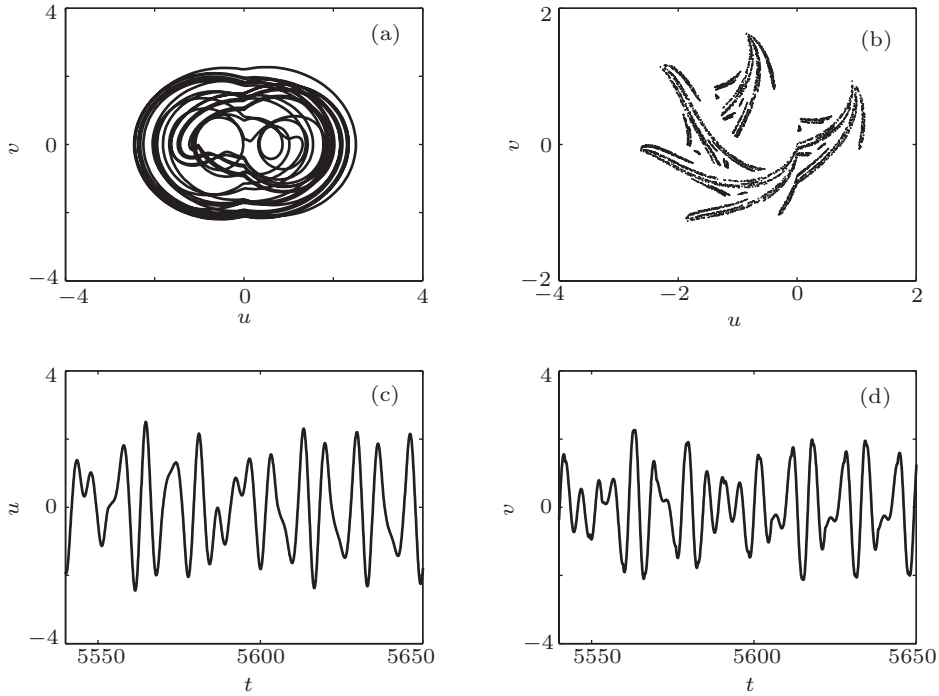


Fig. 13. The chaotic motion for $\alpha = 0$, $\lambda = 0.6$, $\xi = 0.05$, $\Omega = 1.15$, $F = 0.6$.

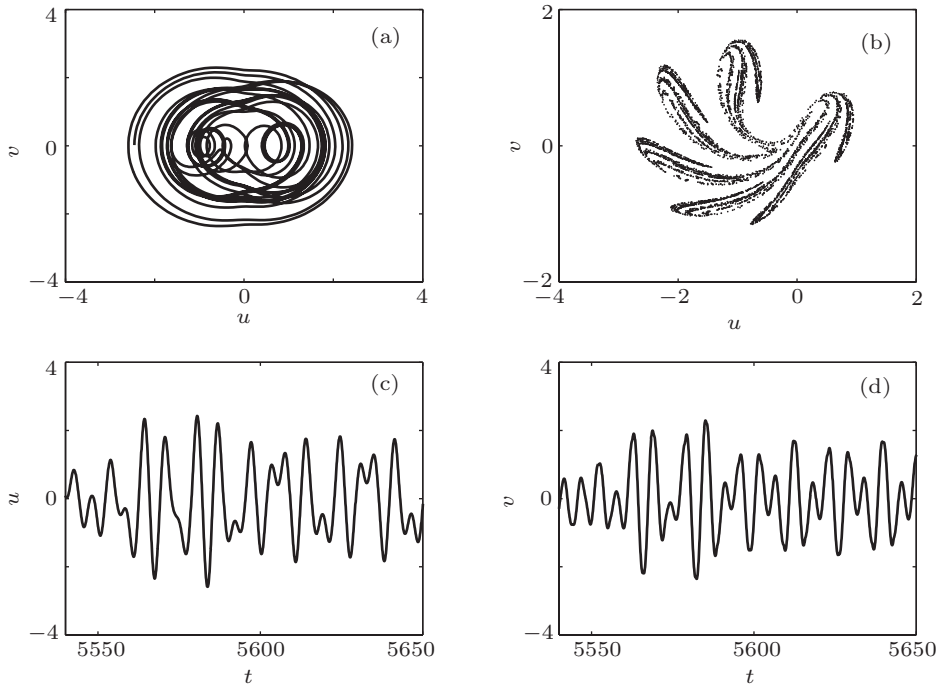


Fig. 14. The chaotic motion for $\alpha = 0.2$, $\lambda = 0.6$, $\xi = 0.05$, $\Omega = 1.15$, $F = 0.5$.

6. Conclusion

In this paper, the global bifurcations and chaos of a system with an irrational restoring force have been investigated directly without using the conventional Taylor's expansion in order to retain the natural characteristics of the system. The nonlinear system presented here include a generalized SD oscillator exhibiting both smooth and discontinuous dynamics depending on the value of a parameter α, while the equilibrium bifurcation depends on the values of parameters α and λ. Furthermore, by introducing a special coordinate transformation, the heteroclinic orbits have been studied in the new coordinates. Then the an-

alytical expressions of unperturbed homoclinic orbits for the original system have been obtained, which enable us to investigate theoretically the chaotic motion of the system for both smooth and the limitedly discontinuous systems. The Melnikov method has been employed to obtain the chaotic boundary, which is in excellent agreement with the numerical investigations. This investigation might be a step towards solving and promote the interest in the open problem proposed in Ref. [1].

References

[1] Cao Q J, Wiercigroch M, Pavlovskaia E E, Thompson J M T and Grebogi C 2008 *Phil. Trans. R. Soc.* A **366** 635

[2] Lai S K and Xiang Y 2010 *Comput. Math. Appl.* **60** 2078

[3] Tufillaro N B, Abbott T and Reilly J 1992 *An Experimental Approach to Nonlinear Dynamics and Chaos* (Boston: Addison-Wesley)

[4] Gimeno E, Álvarez M L, Yebra M S J, Herranz Rosa and Beléndez A 2009 *Int. J. Nonlinear Sci. Numer. Simul.* **10** 493

[5] Mickens R E 1996 *Oscillations in Planar Dynamic Systems* (Singapore: World Scientific)

[6] Sun W P, Wu B S and Lim C W 2007 *J. Sound Vib.* **300** 1042

[7] Cao Q J, Xiong Y P and Wiercigroch M 2011 *J. Appl. Anal. Comput.* **1** 183

[8] Cao Q J, Wiercigroch M, Pavlovskaia E E, Grebogi C and Thompson J M T 2006 *Phys. Rev.* E **74** 046218

[9] Cao Q J, Wiercigroch M, Pavlovskaia E E, Grebogi C and Thompson J M T 2008 *Int. J. Nonlinear Mech.* **43** 462

[10] Tian R L, Cao Q J and Yang S P 2010 *Nonlinear Dyn.* **59** 19

[11] Gatti G, Kovacic I and Brennan M J 2010 *J. Sound Vib.* **329** 1823

[12] Gatti G, Brennan M J and Kovacic Ivana 2010 *Physica* D **239** 591

[13] Beléndez A, Hernández A, Beléndez T, Álvarez M L, Gallego S, Ortuño M and Neipp C 2007 *J. Sound Vib.* **302** 1018

[14] Beléndez A, Beléndez T, Neipp C, Hernández A and Álvarez M L 2009 *Chaos, Solitons and Fractals* **39** 746

[15] Tian R L, Cao Q J and Li Z X 2010 *Chin. Phys. Lett.* **27** 074701

[16] Wiggins S 1983 *Introduction to Applied Nonlinear Dynamical Systems and Chaos* (New York: Springer)

[17] Liu W 1994 *J. Math. Anal. Appl.* **182** 250

[18] Yu W Q and Chen F Q 2010 *Nonlinear Dyn.* **59** 129

[19] Samoylenko S B and Lee W K 2007 *Nonlinear Dyn.* **47** 405

[20] Zhang Y and Bi Q S 2011 *Chin. Phys.* B **20** 010504

[21] Wang W, Zhang Q C and Tian R L 2010 *Chin. Phys.* B **19** 030517

[22] Zhang Q C, Tian R L and Wang W 2008 *Acta Phys. Sin.* **57** 2799 (in Chinese)

[23] Yao M H and Zhang W 2005 *Int. J. Bifur. Chaos* **15** 3923

[24] Jiang G R, Xu B G and Yang Q G 2009 *Chin. Phys.* B **18** 5235

[25] Liang C X and Tang J S 2008 *Chin. Phys.* B **17** 135

[26] Melnikov V K 1963 *Trans. Moscow Math. Soc.* **12** 1

[27] Guckenheimer J and Holmes P 1983 *Nonlinear Oscillation, Dynamical Systems, and Bifurcation of Vector Fields* (New York: Springer)

[28] Chen Y S and Leung A Y T 1998 *Bifurcation and Chaos in Engineering* (London: Springer)